SUPPORTING INFORMATION FOR

Simple host-guest chemistry to modulate the process of concentration and crystallization of membrane proteins by detergent capture in a microfluidic device

Liang Li[1], Sigrid Nachtergaele[1], Annela M. Seddon[1], Valentina Tereshko[2], Nina Ponomarenko[1], Rustem F. Ismagilov[1]*

[1] Department of Chemistry and Institute for Biophysical Dynamics and

[2] Department of Biochemistry and Molecular Biology,

University of Chicago, 929 East 57th Street, Chicago, IL 60637

E-mail: r-ismagilov@uchicago.edu

Chemicals and Materials

All solvents and salts purchased from commercial sources were used as received unless otherwise stated. 1,2,3-Heptanetriol (high melting point isomer), Methyl-β-cyclodextrin (MBCD), and γ-cyclodextrin were purchased from Fluka Biochemika (St. Louis, MO). Lauryldimethylamine oxide (LDAO) and n-Dodecyl-β-D-Maltopyranoside (DDM) were purchased from Anatrace (Maumee, OH). (Tridecafluoro-1,1,2,2,-tetrahydrooctyl)-1 trichlorosilane was obtained from United Chemical Technologies, Inc. (Bristol, PA). Poly(dimethylsiloxane) (PDMS, Sylgard 184 Silicone Elastomer kit) was obtained from Dow Corning (Midland, MI). FC-40 (a mixture of perfluoro-tri-n-butylamine and perfluoro-di-n-butylmethylamine) and FC-70 (perfluorotripentylamine) were obtained from 3M (St. Paul, MN). Chloroform, Ammonium Hydroxide, Methanol, Na_2HPO_4, NaH_2PO_4 and Tris(hydroxymethyl)aminomethane were obtained from Fisher (Fair Lawn,

NJ). Brilliant Blue R was obtained from Sigma- Aldrich (St. Louis, MO). Sodium-3-trimethylsilylpropionate was purchased from Cambridge Isotope Laboratories, Inc. (Andover, MA). D_2O was obtained from Acros Organics (Geel, Belgium). UV-Visible spectrometer was purchased from Agilent (Santa Clara, CA). Teflon tubing (OD 250μm, I.D. 200μm) was purchased from Zeus (Orangeburg, SC). Thirty-gauge Teflon tubing was obtained from Weico Wire & Cable (Edgewood, NY). Standard wall glass tubing was obtained from Chemglass (Vineland, NJ). Gastight syringes were obtained from Hamilton Company (Reno, NV). Amicon Ultra -15 Centrifugal Filter Devices (30K) and Microcon centrifugal filter devices (30K) were purchased from Millipore (Bedford, MA). Partisil K6 60Å TLC Plates (250 μm) were obtained from Whatman (Florham Park, NJ).

Methods

Dynamic Light Scattering Measurement to Characterize Stoichiometric Ratio of MBCD/LDAO Complex Formation. Dynamic light scattering (DLS) was performed at room temperature on a Precision Detectors Inc PD2000 Light Scattering Instrument at 800nm with a scattering angle of 90˚. Samples were prepared in MilliQ water and filtered with a 0.22μM filter before measurement in a 5mm quartz cuvette. The total sample volume was 300μL.

DLS Characterization of Control Samples. Two stock solutions, 300 mM MBCD, 436 mM LDAO were prepared and used to make all subsequent solutions for the control experiments. To identify the size of MBCD and LDAO, 40 mM MBCD and 40 mM

LDAO were measured with DLS. To characterize the stoichiometric ratio of MBCD/LDAO complex formation, LDAO concentration was kept at 40 mM while MBCD concentrations were tested at 20 mM, 40 mM, and 60 mM, yielding LDAO: MBCD ratios of 2:1, 1:1 and 1:1.5.

The sample time was 1μs for free MBCD and 2μs for all other samples. All measurements were collected with a 1s run time, accumulated for 60s, and repeated four times. The data are the cumulative frequency of the particle size for the four runs for each sample.

DLS Characterization of Protein Samples. Reaction Centre from *Blastochloris viridis* was received at 0.15 mM in 3.8 mM LDAO and 50 mM Na_2HPO_4/NaH_2PO_4. Two stock solutions were prepared and used to make all subsequent solutions for samples containing reaction centre: a 100mM solution of MBCD and a 436mM stock solution of LDAO. Four testing samples were prepared by adding stock solutions of LDAO and MBCD to RC sample and diluting with Millipore water to make the final concentration of RC 7.3 μM. The final MBCD/ LDAO concentrations were 0 mM /3.5 mM, 3.5 mM/3.5 mM, 7 mM/3.5 mM, and 1.75 mM/3.5 mM, respectively.

The sample time was 5μs for RC in the absence of MBCD and 10μs for all other samples. All measurements were collected with a 1s run time, accumulated for 60s, and repeated four times. The data are the cumulative frequency of the particle size for the four runs for each sample.

^{1}HNMR Titration Analysis to Characterize the Complex Formation of MBCD/LDAO. To further characterize the formation of MBCD/LDAO complex,

^{1}HNMR titration analysis was performed using D_2O as a solvent. Sodium 3-Trimethylsilylpropionate at 4 mM was used as an internal standard. To identify chemical shifts from MBCD, samples of 1 mM, 2 mM, 6 mM MBCD were measured with NMR. To identify chemical shifts from LDAO, a sample of 2 mM LDAO was measured. For the titration analysis, the LDAO concentration was kept at 2 mM while MBCD concentrations were tested at 0.5 mM, 1 mM, 2 mM, 3 mM, 4 mM, and 8 mM, yielding MBCD: LDAO ratios of 1:4, 1:2, 1:1, 1.5:1, 2:1 and 4:1. The sample of ratio 1.5:1 was re-measured after 72-hour incubation at room temperature.

Fabrication of PDMS Devices. Poly(dimethylsiloxane) (PDMS) was used to fabricate all microfluidic devices. Microchannels with rectangular cross sections were fabricated with rapid prototyping.[1]The channel walls were functionalized with (tridecafluoro-1, 1, 2, 2-tetrahydrooctyl)-1-trichlorosilane to render them hydrophobic and fluorophilic.[2]

Crystallization of RC in the Presence of MBCD or γ - CD. Four aqueous-inlet devices were used to perform the optimization. Precipitant stream was 4M $(NH_4)_2SO_4$, 6.5 mM LDAO in 50 mM Na_2HPO_4/NaH_2PO_4 buffer (pH 6.0); buffer stream was 6.5 mM LDAO; protein stream was 22 mg/mL RC, 3.0 mM LDAO, 4.5% (v/v)TEAP, 7% (w/v)1,2,3-heptanetriol in 50 mM Na_2HPO_4/NaH_2PO_4 buffer (pH 6.0). MBCD stream consisted of an array of plugs of MBCD at concentrations: 0, 28 mM, 56 mM, 112 mM, and 140 mM. MBCD plugs were ~ 50 nL and were separated by air bubbles. The preparation of this array was detailed previously[3]. The carrier fluid was FC-40. All the flow rates were controlled by a Labview subroutine. The protein stream and the MBCD stream were

maintained at constant flow rates of 24 nL/s and 4.2 nL/s, respectively. The flow rate of the precipitant stream was cycled to increase from 20 nL/s to 27 nL/s, and then decrease from 27 nL/s to 20 nL/s, with a step size of 1.7 nL/s. Correspondingly, the buffer stream was cycled to decrease from 10 nL/s to 3.3 nL/s, and then increase from 3.3 nL/s to 10 nL/s, with a step size of 1.7 nL/s. The flow rate of the carrier fluid was cycled to increase from 47 nL/s to 60 nL/s, and then decrease from 60 nL/s to 47 nL/s, with a step of 3.4 nL/s. Each flow rate step lasted for 1.5s. The flow rate change of the carrier fluid was synchronous with the flow rate changes of the aqueous phases. In another similar setup, an array of plugs with γ - CD was used to replace the MBCD stream at the same concentrations.

The trials, in the form of plugs, were transported and stored in Teflon tubing (O.D.: 250 μm and I.D.: 200 μm) which was sealed in glass tubing (O.D.: 3 mm and I.D.: 1.8 mm), prefilled with FC-70.

The experiment was performed under dim light and the trials were kept in the dark at 23 ^{o}C.

Crystal Preparation and X-ray Data Collection. Cryo-protectant for freezing RC crystals was either paraffin oil or 35% (w/v) glucose, 2.6 M $(NH_4)_2SO_4$, 4.4 mM LDAO, 0.5% (v/v) TEAP, 1% 1,2.3-Hepatanetriol in 50 mM Na_2HPO_4/NaH_2PO_4 buffer (pH 6.0). Crystals of RC from *B. viridis* grown in the plugs were extracted by attaching a syringe to one end of the Teflon tubing and flowing the crystals slowly into a drop of cryo-protectant by using the manual syringe driver.[3] Once crystals were flowed into the cryo-protectant drop, the crystals were picked up with a CryoLoop (Hampton Research) and

flash frozen in liquid nitrogen. To determine the space group for all the crystals grown in different MBCD concentrations, the X-ray diffraction experiments were performed at GM/CA Cat station 23 ID-B, BioCars station 14 BM-C and Ls-Cat station 21 ID-D and G of the Advanced Photon Source (Argonne National Laboratory), and the summary of the observed morphologies of the RC crystals is reported in Supporting Table 1. A 10-20^{o} oscillation range was collected and processed in HKL2000[4] to confirm the trigonal or hexagonal symmetry of the crystal. The X-ray data used to solve the new trigonal RC structure reported in Supporting Table 2 were collected at 100 K using a wavelength of 1.0332 Å, an exposure time of 2 s, and an oscillation width of 0.5°. The diffraction data were processed with HKL2000. The trigonal RC crystal form belongs to space group $P3_121$ with cell dimensions $a = b = 241.2$Å, $c = 113.4$Å, $\alpha = \beta = 90^{o}$, $\gamma = 120^{o}$ and diffracts to 3.2 Å resolution. The crystal, used to solve the structure which is discussed in the paper, grew in the presence of 10 mM MBCD and 4.6 mM LDAO.

X-ray Structure Determination of RC. The tetragonal RC crystals were isomorphic to other published RC structures[5,6] and were reported at 1.96 Å resolution by our laboratory using miclofluidic techniques[3] (PDB id 2I5N). The new RC trigonal structure was solved by molecular replacement using PDBid 2I5N structure as a starting model and MOLREP[7] program in CCP4 suite.[8] The rigid-body, positional, and temperature factor refinement was performed using maximum likelihood target with the program REFMAC5.[9] The SigmaA-weighted 2Fobs-Fcalc and Fobs-Fcalc Fourier maps were calculated using CCP4. The Fourier maps were displayed and examined in TURBO-FRODO[10] and COOT.[11] The search for new solvent molecules was performed with help

of COOT. The crystal data, data collection, and refinement statistics are summarized in Supporting Table 2. The coordinates and structure factors have been deposited in the Protein Data Bank with an entry code 3D38 (pending). The RC dimer architecture is found to be similar in the trigonal and tetragonal crystals. Other packing interactions differ in the two crystal forms (Supporting Table 3 and Supporting Figure 4)

Detergent Concentrating and Thin Layer Chromatograph (TLC)

TLC Setup. The preparation of TLC setup followed the reported procedure.[12] Briefly, a 2 L glass beaker was lined with Whatman filter paper and equilibrated with the mobile phase (chloroform: methanol: ammonium hydroxide, 63: 35: 5, v/v/v) for one hour.

DDM Calibration Curve. To check whether TLC could linearly reflect concentration on the plate, 5 μL samples of five separate DDM concentrations were spotted 1.7 cm from the bottom of a 10×20 cm silica gel TLC plate. Once the spotted solution dried, the plate was put into the glass beaker containing the mobile phase. The beaker was then covered with aluminum foil and developed for 80 minutes. The TLC plate was then removed and air-dried before being sealed into a second 2 L beaker, which was prepared by adding iodine crystals and warming in a 60 ^{o}C incubator. After 10-15 minutes of incubation, the TLC plate was removed from the beaker and immediately imaged with a Hewlett-Packard scanner (hp Scanjet 8250). Using *Photoshop 6.0*, the image was first converted to CMYK mode and then changed to grayscale. The detergent spots were quantified with TotalLab TL100. Briefly, an object was drawn around each detergent spot and a copy of each object was drawn adjacent to the detergent spot to obtain the background value. The pixel volume of the background was subtracted from that of the detergent spot. The

obtained values were calibrated by volume, i.e. divided by the solution volume (5 μL), and the resulting value was plotted against the concentration to generate the calibration curve (Supporting Figure 5). The correlation coefficient was 0.9873, indicating a linear correlation between the actual DDM concentration and the intensity of iodine-stained spots.

Concentrating DDM Solutions and TLC Characterization. Two samples, 1) 15 mL 0.51 mM DDM in 20 mM Tris (pH = 7.8) and 2) 15 mL 0.51 mM DDM, 0.51 mM MBCD in 20 mM Tris (pH = 7.8), were concentrated to 650 μL -700 μL. We used two methods to monitor the detergent concentration. First we used a simple assay of UV-visible spectrometry (Supporting Figure 7) and found that during concentration, detergent micelles did not pass the through the membrane and were retained at high concentration in the sample. When equimolar MBCD was added to the sample, the detergent was captured and was able to pass through the membrane, lowering the concentration of detergent remaining in solution. We then performed the TLC experiment using the same procedure as the DDM calibration. Six samples were spotted, from left to right: 1) 15 μL sample 1; 2) 5 μL concentrated sample 1; 3) 15 μL solution that passed through the filter from sample 1; 4) 5 μL concentrated sample 2; 5) 5 μL concentrated sample 2; 6) 10 μL solution that passed through the filter from sample 2 (Supporting Figure 6A). After the TLC experiment, the plate was stained with iodine vapor and imaged with the scanner. The DDM spots were analyzed with TotalLab TL100 in the same manner as described in the DDM calibration above. The obtained values were divided into two groups for analysis: lanes 1, 2 , 3 and lanes 4, 5, 6. The pixel volumes were first calibrated by

volume, and the relative concentration was calculated by defining lanes 1 and 4 as one, for lanes 1, 2, 3 and lanes 4,5,6 respectively. The values are plotted in Figure 3.

Concentrating RC Samples and TLC Characterization

Preparation of RC in DDM. RC in 3.0 mM LDAO and 50mM Na_2HPO_4/NaH_2PO_4 buffer (pH 6.0) was diluted 33 fold in DDM (final DDM concentration 0.51 mM) and 50 mM Na_2HPO_4/NaH_2PO_4 buffer (pH 6.0), and then dialyzed against 200mL of 0.51 mM DDM in 50 mM Na_2HPO_4/NaH_2PO_4 buffer (pH 6.0) at 4˚C for 18 hours in the dark using 10kD cut-off SharkSkin dialysis tubing. The concentration of RC in the dialyzed sample was 0.3 mg/mL, determined using UV-Visible spectroscopy (Agilent 8453).

Concentrating Samples with and without MBCD. Two sets of samples were prepared by adding either 1.5 μL Millipore H_2O (sample I) or 1.5 μL 170 mM MBCD (sample II) to 498.5 μL the dialyzed RC sample. Each had a duplicate. One duplicate from each set was then concentrated with Microcon centrifugal filter devices (30K). The final volume obtained was ~ 20 μL. The concentrations of both samples were measured using UV-Visible spectroscopy at 1/100 dilution (Supporting Figure 8). The concentrations were 8.2 mg/mL and 8.9 mg/mL for samples I and II, respectively.

TLC with Concentrated RC Samples: Five samples were spotted and examined with TLC following the same procedure described in DDM calibration. Five lanes were generated from left to right: 1) 5 μL mixture of 8.3 mM DDM and 218 mM LDAO; 2) 10 μL un-concentrated sample I; 3) 5 μL sample I; 4) 10 μL un-concentrated sample II; 5) 5 μL concentrated sample II. The detergent spots were then quantified with TotalLab TL100. The image of the TLC plate with the drawn objects for quantification is shown in Supporting Figure 6B. The pixel volume of the background was subtracted from that of

the detergent spot. The obtained values were divided into two groups for analysis: lanes 2, 3 and lanes 4, 5. The pixel volumes were first calibrated by volume, and the relative concentration was calculated by defining un-concentrated samples (lanes 2 and 4) as one, for lanes 2,3 and lane 4,5, respectively. The values are plotted in Supporting Figure 7.

Supporting Tables and Figures

Table 1. Summary of RC morphologies in different concentrations of MBCD and LDAO.

[MBCD] (mM)	[LDAO] (mM)	Space group
0	43.6	$P4_32_12$
0	4.6	$P4_32_12$
2	4.6	$P4_32_12$
4	4.6	* $P4_32_12$, $P3_121$
4	5.3	** $P4_32_12$, $P3_121$
8	4.6	$P3_121$
10	4.6	$P3_121$
8 mM γ-CD	4.6	$P4_32_12$

*: All 11 crystals generated in the condition were tested, 2 of which were $P4_32_12$ and 9 of which were $P3_121$. **: 6 crystals generated in the condition were tested, 1 of which was $P3_121$ and 5 of which were $P4_32_12$.

Table 2. Data collection and refinement statistics of RC trigonal crystals.

	Microfluidic hybrid method
Data collection	
Space group	$P3_121$
Cell dimensions	
a, *b*, *c* (Å)	241.2, 241.2,113.4
α, β, γ (°)	90, 90, 120
Resolution (Å)	50- 3.2
R_{merge}	0.168
$I/\sigma I$	5.8
Completeness (%)	99.8
Redundancy	6
Refinement	
Resolution (Å)	50-3.2
No. reflections	62025
R_{work}/ R_{free}	0.192 / 0.224
No. atoms	
Protein	9290
Ligand	785

Fe / Mg /SO_4 ions	5 / 4 / 15
Water	158
B-factors	
Protein	67.8
Ligand	
Fe / Mg /SO_4 ions	67.8 / 41.4 / 81.5
Water	58.9
R.m.s deviations	
Bond lengths (Å)	0.012
Bond angles (°)	1.437

Table 3: Summary of residues involved in forming protein contacts in Tetragonal and Trigonal RC crystals.

Tetragonal RC	Trigonal RC
Chain C 71L, 72R, 75T, 78T, 83P, 84Q, 85E, 86G, 87C, 88T, 92D, 93E, 94N, 200Q, 211L, 212V, 213G, 214V, 216R, 218K, 219E, 21 residues.	**Chain C** 14F, 15R, 37Q, 83P, 84Q, 93E, 94N, 157R, 159T, 162H, 165R, 167E, 168T, 256W, 257G, 292S, 293R, 17 residues.
Chain H 1M, 26T, 29L, 30L, 33R, 34R, 37R, 56D, 59V, 60Y, 61E, 64Y, 138R, 141T, 151D, 153R, 154G, 155L, 164E, 167T, 168V, 186S, 189G, 250T, 251P, 252E, 255E, 256S, 28 residues.	**Chain H** 2Y, 29L, 30L, 33R, 34R, 37R, 56D, 59V, 60Y, 61E, 64Y, 11 redidues.
Chain L 12R, 18G, 19G, 20D, 4 residues.	**Chain L** 57P, 73Y, 79P, 81L, 82E, 5 residues.
Chain M 323K, 1 residue.	**Chain M** 298K, 306P, 307A, 308Y, 309L, 310P, 311A, 312T, 313P, 314D, 317S, 318L, 319P, 13 residues.

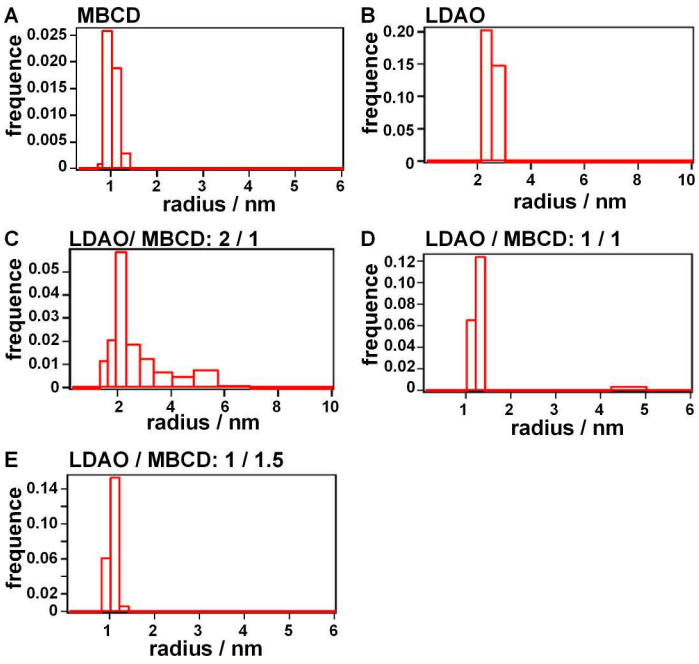

Figure 1. Size distribution radii of LDAO and MBCD measured by dynamic light scattering (DLS). (A) 40mM MBCD; (B) 40mM LDAO; (C) 40mM LDAO: 20mM MBCD (2:1 molar ratio); (D) 40mM LDAO: 40mM MBCD (1:1 molar ratio); (E) 40mM LDAO: 60mM MBCD (1:1.5 molar ratio). Published values for LDAO = 2 nm;[13] MBCD = 0.78nm.[14]

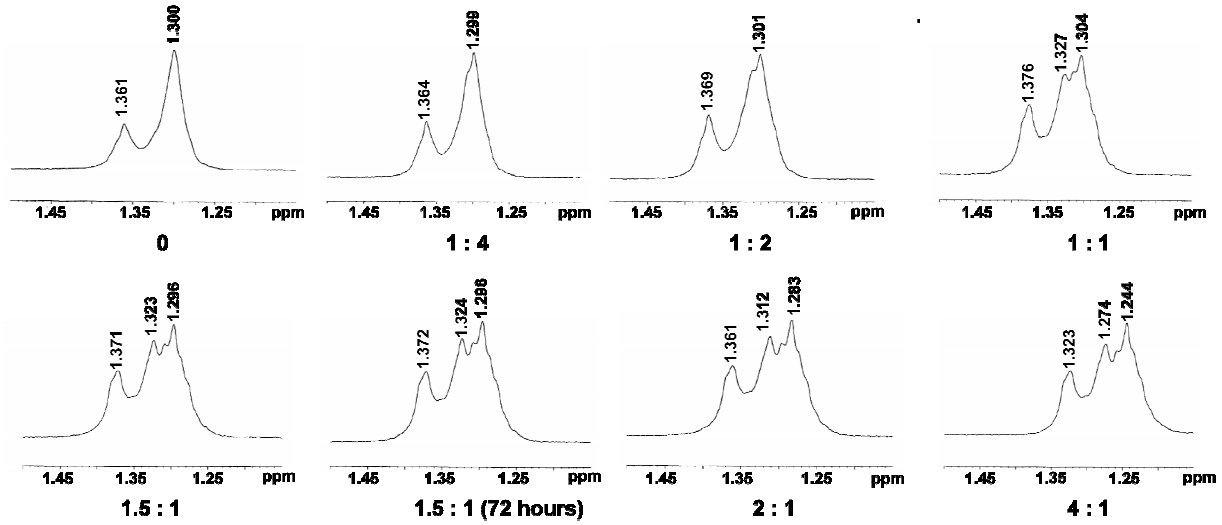

Figure 2. Segments of ^{1}HNMR spectra corresponding to C3-C10 of LDAO. Different MBCD: LDAO ratios are indicated below each spectrum. Peak splitting seen at 1.30 ppm did not change when ratios of MBCD:LDAO reached 1:1 or greater, thus supporting the formation of 1:1 complex observed in characterization of the MBCD:LDAO by DLS.

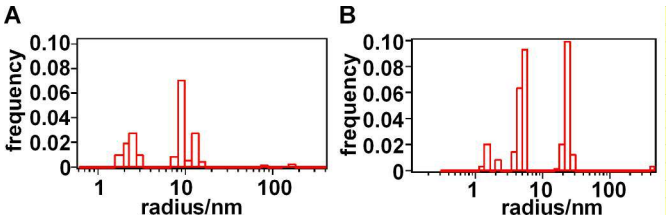

Figure 3: DLS characterization of RC samples with insufficient (A) and excessive (B) detergent extraction. (A) ~ 7.3 μM RC, 1.8 mM MBCD in 3.5 mM LDAO, 25 mM NaH_2PO_4-Na_2HPO_4, pH=6.0; (B) ~ 7.3 μM RC, 7 mM MBCD in 3.5 mM LDAO, 25 mM NaH_2PO_4-Na_2HPO_4, pH=6.0;

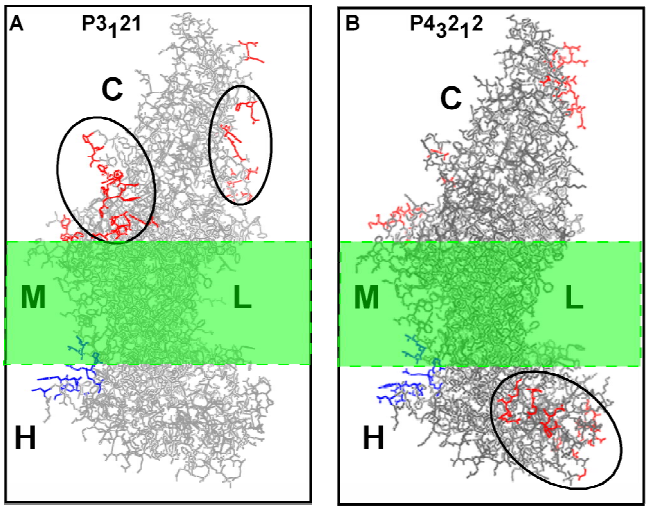

Figure 4: Different RC residues (circled in black) are involved in the packing interactions in trigonal (A) and tetragonal (B) crystals. The close contacts between the symmetrically related RC molecules were identified using CONTACT/ACT program (CCP4 program Suite 6.0.1/Structure analysis/Analyse Molecular Contact) within 5 Å. The hydrophobic parts of RC are covered by transparent green. Subunits C, H, M and L are indicated in the figure. The residues of subunit H that mediate the formation of the crystallographic 2-fold RC dimer are the same in both crystal forms and are shown in blue (residues L29, L30, R33, R34, R37, D56, V59, Y60, E61, Y64). (A) Trigonal $P3_121$ crystal form crystals grown in the presence of 10 mM of MBCD. The subunit C residues involved in the new packing contacts around 3_1 crystallographic *c*-axis account for ~ 600 $Å^2$ of the buried area and are circled in black. The residues are: F14, R15, Q37 P83, Q84, R157, T159, H162, R165, E167, T168, W256, G257, S292, R293; (B) Tetragonal $P4_32_11$ crystal form grown in the absence of MBCD. The subunit H residues involved in the crystal packing around 2_1 crystallographic *b*-axis present in $P4_32_12$ space group account for ~ 300 $Å^2$ of the buried area and are lost in the trigonal crystals and are circled in black. The residues are: R138, T141, D151, R153, G154, L155, E164, T167, V168, S186, G189,

T250, P251, E252, E255, S256 and 4 residues from subunit L (R12, G18, G19, and D20). The contacts around crystallographic 4_3 *c*-axis formed by subunit C residues account for ~ 400 Å^2 of the buried area that is smaller than 600 Å^2 found in trigonal crystals (A) and are shown in red on top. The residues are: L71, R72, T75, T78, P83, Q84, E85, G86, C87, T88, D92, E93, N94, Q200, L211, V212, G213, V214, R216, K218 and E219. Comparing A and B, the buried area of trigonal crystals (~ 600 Å^2) is slightly smaller than the total buried area of tetragonal crystals (~ 700 Å^2). The buried areas in protein contacts were analyzed using *AreaIMol* program (CCP4 program Suite 6.0.1/Structure analysis/Analyse Accessible Surface Areas). Contact areas by residues were recorded, and the total area from the contacts was calculated.

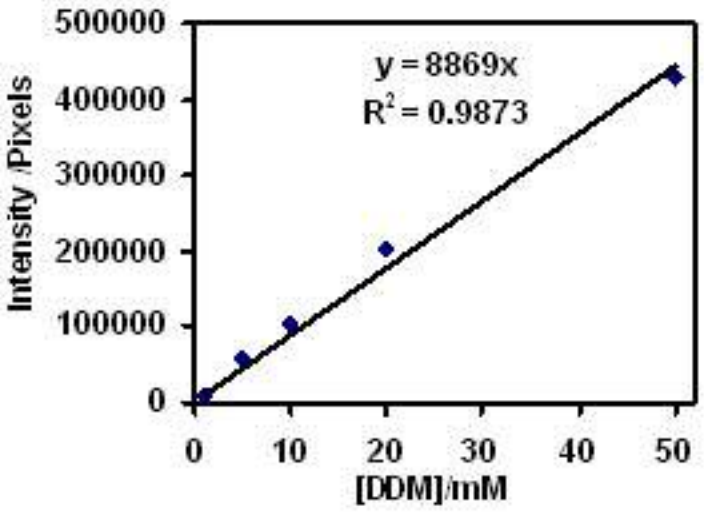

Figure 5: Calibration curve of DDM determined in one TLC plate. The curve had a linear fitting with intercept at zero, and the correlation coefficient was 0.9873.

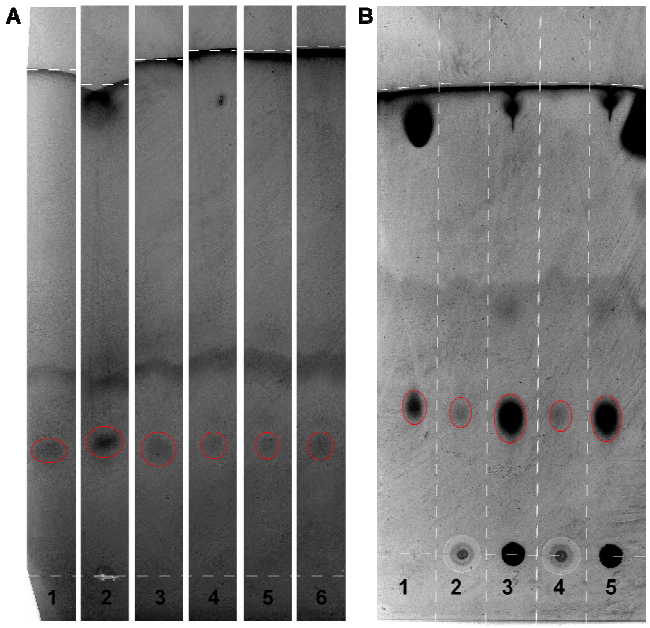

Figure 6: Images of iodine stained TLC plates in gray scale. The spots analyzed with TotalLab TL100 are circled in red. (A) TLC of solutions obtained from concentrating DDM solutions of two groups: without MBCD (lanes 1,2,3) and with MBCD (lanes 4,5,6). In each group, the left lane is the original sample, the middle lane is the concentrated sample and the right lane is the solution passing through the membrane of the concentrator. (B) TLC of RC samples from two groups: without MBCD (lanes 2,3) and with MBCD (lanes 4,5). In each group, the left lane is the original sample and the right lane is the concentrated sample. Lane one was loaded with a mixture of LDAO and DDM.

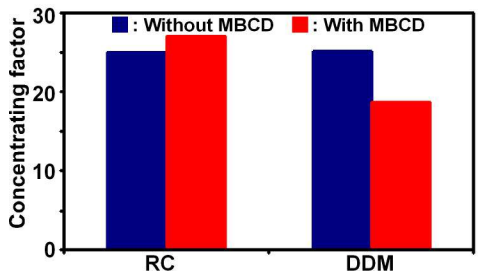

Figure 7: MBCD was used to minimize the concentration of detergent micelles during protein concentration. There was an increase in relative concentration of both RC and DDM when samples of RC in DDM were concentrated. RC concentration increased ~ 25 times both without (25 times) and with (27 times) MBCD; [DDM] increased 25 times when no MBCD was present while its increase was reduced to 19 times when equimolar MBCD to DDM in buffer was added. DDM in RC sample could be divided into four groups: 1) DDM monomers; 2) DDM forming free micelles; 3) DDM tightly bound to RC; and 4) DDM loosely bound to RC. C_{mono}, C_{mic}, C_{tight} and C_{loose} denote these concentrations respectively. During the process of concentration without MBCD, the starting concentration should be $C_{start1} = (C_{mono} + C_{mic} + C_{tight} + C_{loose})$, and the final concentration should be $C_{final1} = (C_{mic} + C_{tight} + C_{loose}) \times X = (C_{start1} - C_{mono}) \times X$, assuming the protein is concentrated by a factor of X and only monomers can pass through the filter. During the process of concentration with MBCD, the starting concentration of DDM should be $C_{start2} = C_{start1} = (C_{mono} + C_{mic} + C_{tight} + C_{loose})$, and the final concentration should be $C_{final2} = C_{tight} \times X = (C_{start2} - C_{mono} - C_{mic} - C_{loose}) \times X$, assuming MBCD binds to DDM from monomers, micelles and the ones loosely bound to proteins and passes through the filter. As a result, the final concentration of DDM in the concentrated sample in the presence of MBCD, C_{final2}, is smaller than the final concentration of DDM in the absence of MBCD. The difference is $(C_{final1} - C_{final2}) / C_{final2}$

= (C_{mic} + C_{loose}) / C_{tight}. Most detergents are tightly bound to protein and cover the hydrophobic belt of the protein, so usually C_{tight} is bigger than (C_{mic} + C_{loose}). In other words, the difference, (C_{final1} - C_{final2}) / C_{final2}, should be less than one. In our test, it was 0.3. Thus, in the process of concentration of RC, MBCD captured micellar DDM and passed through the filter. However, most DDM was tightly bound to RC; this DDM also became concentrated together with RC.

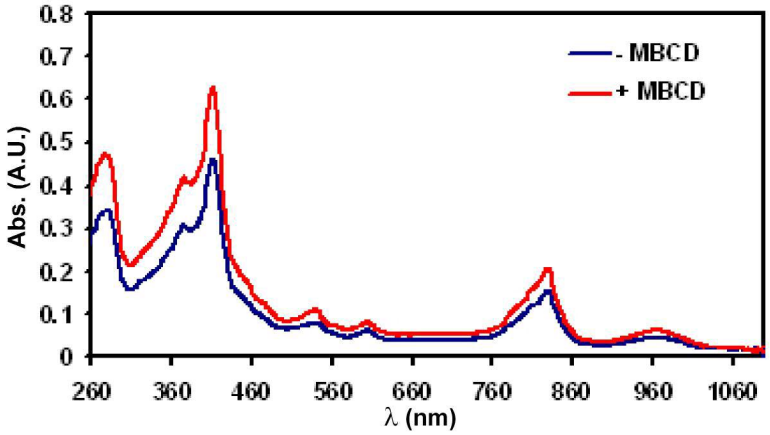

Figure 8: UV-visible spectra of RC after concentration with MBCD (in red) and without MBCD (in blue). The peaks of absorbance of both samples were identical to each other, and the difference in intensity was due to the difference in concentration. This observation indicated that the addition of MBCD during the concentrating process did not alter the optical property of RC.

References

(1) D.C. Duffy, J.C. McDonald, O.J.A. Schueller, G.M. Whitesides, *Anal. Chem.* 1998, **70**, 4974

(2) L.S. Roach, H. Song, R.F. Ismagilov, *Anal. Chem.* 2005, **77**, 785

(3) Li, L.; Mustafi, D.; Fu, Q.; Tereshko, V.; Chen, D. L. L.; Tice, J. D.; Ismagilov, R. F. *Proc. Natl. Acad. Sci. U. S. A.* **2006**, *103*, 19243-19248.

(4) Otwinowski, Z.; Minor, W. In *Macromolecular Crystallography, Pt A*; ACADEMIC PRESS INC: San Diego, 1997; Vol. 276, pp 307-326.

(5) Baxter, R. H. G.; Seagle, B. L.; Ponomarenko, N.; Norris, J. R. *Acta Crystallogr. Sect. D-Biol. Crystallogr.* **2005**, *61*, 605-612.

(6) Deisenhofer, J.; Epp, O.; Sinning, I.; Michel, H. *Journal of Molecular Biology* **1995**, *246*, 429-457.

(7) Vagin, A.; Teplyakov, A. *Journal of Applied Crystallography* **1997**, *30*, 1022-1025.

(8) Collaboration *Acta Crystallogr. D, Biol. Crystallogr. (Denmark)* **1994**, *D50*, 760-763.

(9) Murshudov, G. N.; Vagin, A. A.; Dodson, E. J. *Acta Crystallogr. Sect. D-Biol. Crystallogr.* **1997**, *53*, 240-255.

(10) Cambillau, C.; Roussel, A. *Turbo Frodo, version OpenGL.1*; University Aix-Marseille II: Marseille: Marseille, 1997.

(11) Emsley, P.; Cowtan, K. *Acta Crystallogr. Sect. D-Biol. Crystallogr.* **2004**, *60*, 2126-2132.

(12) Eriks, L. R.; Mayor, J. A.; Kaplan, R. S. *Analytical Biochemistry* **2003**, *323*, 234-241.

(13) Thiyagarajan, P.; Tiede, D. M. *Journal of Physical Chemistry* **1994**, *98*, 10343-10351.

(14) Gonzalez-Gaitano, G.; Rodriguez, P.; Isasi, J. R.; Fuentes, M.; Tardajos, G.; Sanchez, M. *Journal of Inclusion Phenomena and Macrocyclic Chemistry* **2002**, *44*, 101-105.